Biolistic Loading of Voltage-Sensitive Dyes into Cells in Rat Brain Slices for Optical Recording of Neuron Activity

ARTICLE *in* NEUROSCIENCE AND BEHAVIORAL PHYSIOLOGY · MARCH 2013

DOI: 10.1007/s11055-013-9734-z

5 AUTHORS, INCLUDING:

Nikolay Aseyev

7 PUBLICATIONS **13** CITATIONS

SEE PROFILE

Evgeny Nikitin

Russian Academy of Sciences

29 PUBLICATIONS **255** CITATIONS

SEE PROFILE

Matvey Roshchin

Russian Academy of Sciences

11 PUBLICATIONS **16** CITATIONS

SEE PROFILE

Pavel Balaban

Institute of Higher Nervous Activity and Ne…

202 PUBLICATIONS **1,365** CITATIONS

SEE PROFILE

Journal of Neuroscience Methods 212 (2013) 17–27

Contents lists available at SciVerse ScienceDirect

Journal of Neuroscience Methods

journal homepage: www.elsevier.com/locate/jneumeth

Basic Neuroscience

Biolistic delivery of voltage-sensitive dyes for fast recording of membrane potential changes in individual neurons in rat brain slices

Nikolay Aseyev*, Matvey Roshchin, Victor N. Ierusalimsky, Pavel M. Balaban, Evgeny S. Nikitin

Institute of Higher Nervous Activity and Neurophysiology of Russian Academy of Sciences, Butlerova 5A, Moscow 117485, Russian Federation

HIGHLIGHTS

- Biolistic delivery allowed rapid staining with hydrophobic voltage-sensitive dyes.
- The dyes di-12-ANEPPQ and di-8-ANEPPS stained the neuronal soma, dendrites and axon.
- Biolistic delivery provided the fluorescence suitable for fast voltage imaging.

GRAPHICAL ABSTRACT

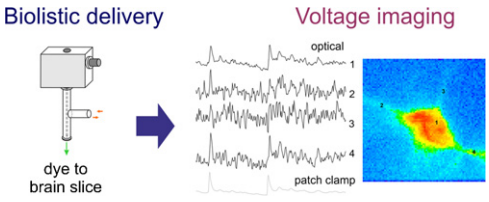

ARTICLE INFO

Article history:
Received 21 July 2012
Received in revised form 3 September 2012
Accepted 5 September 2012

Keywords:
Biolistic delivery
Voltage-sensitive dyes
Optical recording
Neuron
Membrane
Brain slices

ABSTRACT

Optical recording of membrane potential changes with fast voltage-sensitive dyes (VSDs) in neurons is one of the very few available methods for studying the generation and propagation of electrical signals to the distant compartments of excitable cells. The more lipophilic is the VSD, the better signal-to-noise ratio of the optical signal can be achieved. At present there are no effective ways to deliver water-insoluble dyes into the membranes of live cells. Here, we report a possibility to stain individual live neurons with highly lipophilic VSDs in acute brain slices using biolistic delivery. We tested four ANEP-based VSDs with different lipophilic properties and showed their ability to stain single neurons in a slice area of up to 150 μm in diameter after being delivered by a biolistic apparatus. In the slices of neocortex and hippocampus, the two most lipophilic dyes, di-8-ANEPPS and di-12-ANEPPQ, showed cell-specific loading and Golgi-like staining patterns with minimal background fluorescence. Simultaneous patch-clamp and optical recording of biolistically stained neurons demonstrated a good match of optical and electrical signals both for spontaneous APs (action potentials) and stimulus-evoked events. Our results demonstrate the high efficiency of a fast and targeted method of biolistic delivery of lipophilic VSDs for optical signals recording from mammalian neurons in vitro.

1. Introduction

Voltage imaging in live neurons plays a central role in resolving scientific problems in modern neuroscience at many levels, providing a unique tool to probe the membrane potential from the level of single cellular compartments up to the scale of large brain areas with many neuronal networks. Although these methods were extensively used and developed during decades of research (Cohen and Salzberg, 1978), they still present a significant technical challenge to acquire an appropriate optical recording of the neurons in a specific preparation (Peterka et al., 2011). One of the main problems is to choose a right sensor which provides the best sensitivity of recording for the chosen object, and at the same time causes minimal side effects such as photodamage, phototoxicity, dye internalization, dye leak, non-uniform staining or undesired pharmacological effects. For most preparations the correct choice could be made only empirically (Ross and Reichardt, 1979; Tsau

Abbreviations: ANEP-based dyes, aminonaphthylethenylpyridinium-based dyes; AP, action potential; ASCF, artificial cerebrospinal fluid; CCD camera, charge-coupled device camera; DIC, differential interference contrast; N.A., numerical aperture; ROI, region of interest; RT, room temperature; S/N ratio, signal-to-noise ratio; VSD, voltage-sensitive dye; LSM, laser scanning microscope; LED, light emitting diode; fps, frames per second.

* Corresponding author. Tel.: +7 495 3344151; fax: +7 499 7430056.
E-mail address: aseyev@ihna.ru (N. Aseyev).

0165-0270/$ – see front matter © 2012 Elsevier B.V. All rights reserved.
http://dx.doi.org/10.1016/j.jneumeth.2012.09.008

et al., 1996; Vignali et al., 2010). To minimize possible side effects, the VSDs are frequently used at the lowest possible concentrations to provide the acceptable sensitivity and meet the minimal requirements of spatiotemporal resolution. Many attempts were dedicated to improve the methods of voltage imaging via synthesis of potentially better dyes (Acker et al., 2011; Theer et al., 2011), development of new imaging equipment (Bouevitch et al., 1993; Nishimura et al., 2006), or suggesting completely new approaches (Kralj et al., 2012; Miller et al., 2012). In the present study we introduce a new technique of loading neurons in rat brain slices with highly sensitive lipophilic VSDs that are undeliverable by conventional means.

Acute brain preparations and slices are commonly used for in vitro study of mammalian brain functions (Ballanyi, 1999) and optical imaging (Cohen, 1988; Canepari and Zecevic, 2010). Water-soluble fluorescent ANEP-based VSDs, like di-1-ANEPPS (JPW3028), di-2-ANEPEQ (JPW1114) or di-4-ANEPPS, are often chosen for intracellular loading and bath-application in cortical slices (Grinvald et al., 1987; Antic et al., 1997; Foust et al., 2011; Palmer and Stuart, 2006; Sinha and Saggau, 1999; Tominaga et al., 2000). However, a series of lipophilic VSDs with significantly higher sensitivity to membrane potential changes has been synthesized (Tsau et al., 1996). The highly hydrophobic characteristics of the new dyes reduce the number of possible applications to mostly retrograde loading through the distal neurites within peripheral ganglia (Grinvald et al., 1987; Vignali et al., 2010; Wenner et al., 1996; Wu et al., 1998). Reported successful examples of loading of hydrophobic dyes by injection or bath application have used moderate concentrations of surfactants (Pluronic F-127 in DMSO) to improve dye solubility (Obaid et al., 1999; Stein et al., 2011) but with a likely adverse effect on normal cell physiology. Bath application of dyes was successfully used in cortical slices for recording the population activity in large networks, but single-cell resolution was unattainable (Peterka et al., 2011) mostly because of small cell size and dye diffusion and internalization that greatly increased the background intensity. As a result intracellular injection remains the only suitable way of dye delivery for optical recording of single cells and cellular compartments in acute brain slices. The loading technique through the patch pipette was successfully used with water soluble VSDs revealing voltage changes even in small neuronal compartments like presynaptic buttons and dendritic spines (Foust et al., 2011; Palmer and Stuart, 2009). To load a cortical neuron with a VSD by conventional protocol (Antic et al., 1999) one needs to first deliver it into the cell through the patch pipette and then to repatch the cell with a dye-free pipette to control the electrical properties of the membrane during optical recording. Adding to the complexity of the method, a successful loading and incubation with di-2-ANEPEQ or its analogs should be performed at room temperature (RT) (Antic et al., 1999). After incubation, the cells are repatched and recorded at RT or lower (Palmer and Stuart, 2006; Volgushev et al., 2011) or the temperature in the slice chamber must be increased to physiological levels (34–36 °C) immediately before repatching and imaging (Foust et al., 2010; Popovic et al., 2011). During the staining procedure, some amount of dye may leak out of the pipette and stain elements near the recorded cell, thus increasing the background fluorescence and masking the optical signals from thin neurites (Zhou et al., 2007). Thus, the technique of dye loading through the pipette has many complications restricting its routine use. Two possible ways were considered to improve the dye delivery to distant neuronal compartments: the use of more soluble ANEP dyes and cyclodextrin polymer rings as carriers of molecules of lipophilic VSDs instead of conventional surfactants (Antic et al., 1999). Dyes with increased solubility have been successfully employed recently (Zhou et al., 2007), but to the best of our knowledge, no experimental evidence has been presented that confirms the new polymer surfactants are more efficient for VSD delivery.

In the present study, we loaded the neurons of rat brain slices with highly sensitive lipophilic VSDs by applying a technique of biolistic delivery. The biolistic delivery was first introduced for transformation of cells with genetic vectors several decades ago (Sanford, 1988), and was recently shown to be applicable for morphological staining of live and fixed tissues with lipophilic carbocyanine and dextran-based dyes (Gan et al., 2000, 2009; Lichtman et al., 2008; Morgan and Kerschensteiner, 2011; Seabold et al., 2010). This technique was also used to deliver calcium sensitive probes in brain slices and mouse brains in vivo (Kettunen et al., 2002). Several recent key modifications of the apparatus of biolistic delivery decreased the harm of pneumatic impact and permitted its use in acute brain slices (O'Brien et al., 2001; Rinberg et al., 2005; Shefi et al., 2006). Using a custom-made device (Aseyev et al., 2012) designed and fabricated by adapting published principles and schemes we tested a range of 4 different ANEP-based VSDs varying the lipophilic properties of the probe to find the best candidate for neuronal staining with biolistic delivery. Here we report the two most lipophilic dyes, di-8-ANEPPS and di-12-ANEPPQ, provide cell-specific loading and Golgi-like staining patterns with minimal background intensity. Simultaneous patch-clamp and optical recordings of stained cells showed excellent optical signal for imaging of both spontaneous APs and stimulus-evoked events in single neurons.

2. Materials and methods

2.1. Preparation of brain slices

All experimental protocols were performed in accordance with the National Institutes of Health Guide for the Care and Use of Laboratory Animals and approved by the Department of Humanitarian Expertise and Bioethics of RAS. Wistar rats (15–21 days old) were deeply anaesthetized with diethyl ether and decapitated. Brains were rapidly removed and placed in ice-cold ACSF. Brain slices (300 μm) were cut using a vibratome VT1200S (Leica, Germany) from the primary visual cortex of right hemisphere or hippocampus. ACSF contained (in mM): 125 NaCl, 25 $NaHCO_3$, 27.5 glucose, 2.5 KCl, 1.25 NaH_2PO_4, 2 $CaCl_2$ and 1.5 $MgCl_2$ (all Sigma Ultra graded), pH 7.4 and aerated with 95% O_2, 5% CO_2 (details in Volgushev et al., 2000). The slices were incubated at RT for at least 1 h 30 min before the experiments.

2.2. Patch-clamp recording

Patch pipettes were pulled on a horizontal puller P-97 (Sutter Instruments, Novato, CA, USA) from borosilicate glass (GB 150F-8P, Science Products GmbH, Germany) with a tip resistance of 6–7 MΩ. Patch pipettes were filled with a solution containing (in mM) 132 K-Gluconate, 20 KCl, 4 Mg-ATP, 0.3 Na_2GTP, 10 Na-Phosphocreatine, 10 HEPES, pH 7.25 (all from Sigma, St. Louis, MO, USA). Alexa Fluor 488 hydrazide (100 μM, Invitrogen, Carlsbad, CA, USA) was added to the pipette solution for double labeling of the recorded cells in control experiments. Pre-selection of stained pyramidal neurons for recording was performed using Nomarski DIC optics and infrared videomicroscopy. Membrane potential was recorded in whole-cell current clamp mode with an amplifier ELC-03XS (NPI Electronic GmbH, Germany), low-pass filtered at 3 kHz and sampled at 5 kHz with DigiData 1440A running under the Axoscope 10 software (both from Molecular Devices, Sunnyvale, CA, USA). For precise positioning of the patch pipette, the rig was equipped with a motorized micromanipulator Junior (Luigs and Neumann, Germany) mounted on an air table (Scientifica, UK). The whole rig

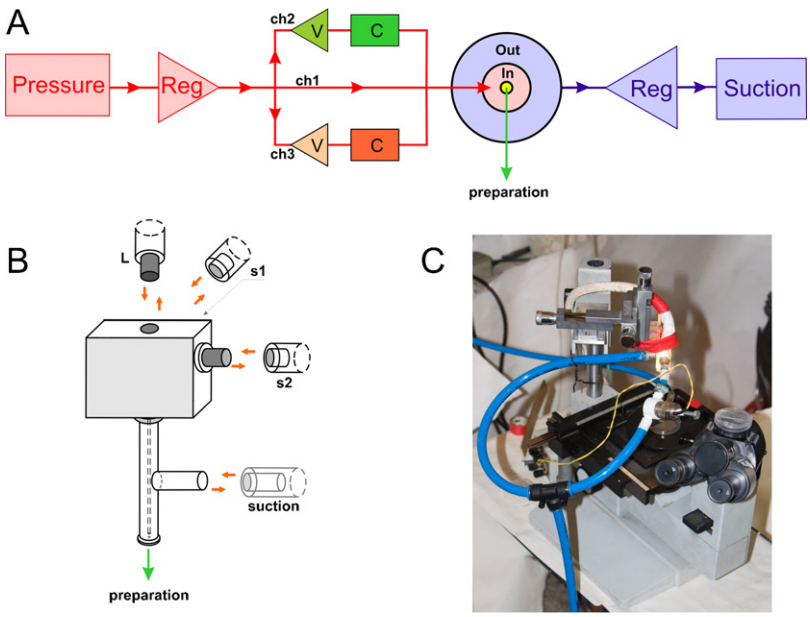

Fig. 1. Custom made device for biolistic delivery of VSDs. (A) Scheme of a two-channel biolistic device powered by pressure and continuous active suction. *Pressure* – source of high pressure (compressed helium or air); *Reg* – pressure regulator; *C*, two independent loading chambers; *V*, electronic valves to control the loading chambers; *In*, inner tube (barrel); *Out*, outer tube for the negative pressure supply provided by a vacuum pump with a pressure regulator *Reg.*; *L*, *s1*, *s2* – fittings for tubing connection to the inputs of the biolistic device. (B) Scheme of biolistic head unit with gas mixer chamber and barrel. Green arrow shows the direction of biolistic shot. (C) Full view of biolistic device for staining with VSDs mounted on the stage of an inverted microscope for manipulating with acute brain slices. (For interpretation of the references to color in this figure legend, the reader is referred to the web version of the article.)

was shielded by a grounded Faraday cage. During recording the slices were kept at RT ($22 \pm 2\,^{\circ}C$) and perfused at a constant rate of 3 ml/min with the aerated ACSF.

2.3. Biolistic device

Neuron staining with VSDs was accomplished using a biolistic delivery of microprojectiles coated with the dye. The biolistic device was custom made to minimize the damage to the brain slices by adapting the published principles and schemes (Rinberg et al., 2005; Shefi et al., 2006). We employed active vacuum suction and 150 μm focusing aperture as described previously (Aseyev et al., 2012). The device was controlled with a hand-operated manipulator mounted on the stage of an inverted microscope (Biolam-P1, LOMO, Russia). We used an optically guided aiming of biolistic delivery at target preparation with a harmless red laser or light spot of a halogen lamp projected through the output tube and aligned along the trajectory line of the biolistic shot (Fig. 1). An 8 cm long inner channel of the device consisted of a glass tube with the inner diameter of 0.58 mm while the outer tube was made of a polypropylene syringe of 6 mm outer diameter. Mixing and loading chambers were custom made of Plexiglass as a single part where the tube holder was threaded into the opening while its pneumatic connection was glued to the Luer-lock with a two component glue. High-pressure fittings and tubings (Festo, Brussels, Belgium) were used for the connection of pneumatic pressure supply with other components. For user-controlled triggering of microprojectiles-loaded pneumatic channel we used an electrical solenoid valve (Aalborg, Orangeburg, NY, USA) driven by a waveform generator AFG320 (Tektronix, Beaverton, OR, USA). Active suction was provided by a vacuum pump VE-160 (170 l/min, P_r 5 Pa, PRC). The operating pressure was kept at around 4.2 bar (62 psi) to avoid ripples on the surface of the ACSF that covered the preparation and was 2 mm from the output opening of the biolistic device. The gap between the inner output tube and the outer tube (Fig. 1A and B) was empirically adjusted to ~0.8 mm to make the active suction more efficient and provide wider scattering of microprojectiles. The way of application of suction, distance to the preparation, and length of the inner tube were the most important parameters to determine the depth of penetration and scattering pattern of the microprojectiles.

2.4. Coating of microprojectiles with VSDs

We tested a range of 4 different ANEP-based voltage-sensitive dyes with increasing lipophylic properties (dye screening in Rohr and Salzberg, 1994). The dyes di-2-ANEPEQ (JPW1114), di-4-ANEPPS (JPW211), and di-8-ANEPPS (JPW1153) are commercially available from Invitrogen (Carlsbad, CA, USA). di-12-ANEPPQ was kindly provided by Leslie M. Loew (University of Connecticut Health Center, Farmington, CT), also available from Biotium. In addition, we used di-1-ANEPPQ (JPW3027, a close analog of JPW3028 and JPW1114, provided by L.M. Loew) in control experiments with dye loading through the patch pipette. To coat the microprojectiles with a VSD we dispersed about 20 mg of 1.6-μm-sized gold particles (BioRad Laboratories, Hercules, CA, USA) evenly on the top of a microscope slide and washed them with a solution of the VSD dissolved in dichloromethane at the concentration of 2.5 mg/ml. As an application of a highly volatile solvent of dichloromethane quickly evaporated, the coated particles could be scraped off with a sharp blade. The particles were then suspended in 1 ml H_2O, sonicated for 5 min (80% cycle, maximum power) with Sonoplus HD-2070 (Bandelin, Germany), and air dried in the dark. Coated particles were stored at $4\,^{\circ}C$ in tightly closed light-protected tubes. For the experiment one tube with microprojectiles was warmed to RT and shaken well before use.

2.5. Biolistic delivery protocol

A small number (less than 0.5 mg in total weight) of VSD-coated microprojectiles was picked up by the tip of a broken glass microelectrode and placed into the loading chamber of biolistic apparatus before each experiment. The brain slice was gently moved from the incubator onto a plastic Petri dish, positioned

under the biolistic device, and highlighted with a targeting light spot. The slice remained in the dish only for 2–3 min in the oxygenized ASCF while it was immobilized with a grid of nylon threads attached to a silver ring.

We aimed the biolistic device at the slice area using laser targeting under control of the inverted microscope focused on the slice. The output tube of the biolistic device was slowly lowered until the barrel end was 2 mm from the slice. To release the microprojectiles, we triggered the solenoid valve with externally generated current steps of 50 ms duration unless otherwise stated. After the biolistic shot we immediately transferred the slices under the recording microscope to image the delivery pattern of microprojectiles or to perform patching and potential recording with a fast CCD-camera.

2.6. Arrangement of the recording apparatus

For optical imaging and patch-clamp recording we used an upright microscope (Olympus BX51WI) equipped with infrared differential interference contrast optics (IR-DIC) and fast NeuroCCD-SM camera (RedShirtImaging, Decatur, GA, USA) operated under control of the NeuroPlex software (RedShirtImaging). The excitation was controlled with an externally mounted shutter (35 mm, Uniblitz, Rochester, NY, USA). Current steps were programmed and triggered with an electronic pulse-generator Master-8 (AMPI, Israel). We stimulated the stained neurons either with 10 Hz trains of short (2–3 ms) current steps of higher amplitude (1–2 nA) or with single long steps of 0.4–0.5 nA. The resting membrane potential was decreased to about −70 mV by a negative current injection. The amplitude of stimulating current was adjusted to evoke single APs.

2.7. Imaging

We excited the fluorescent VSDs with a 150 W xenon arc lamp powered by a ripple-noise protected power supply (Opti-Quip, Highland Mills, NY, USA) mounted on the microscope equipped with a water-immersion objective (Olympus LUMPlanFL 40×/0.8 NA). The filter cubes were selected for the optimal bandpass (Tsau et al., 1996) of excitation at 500–550 nm (HQ 525/50X, Chroma Technology, Bellows Falls, VT, USA) and emission 600 nm, lowpass (3RD600LP, Omega Optical, Brattleboro, VT, USA). For data acquisition, synchronization, and programming of TTL signals we used the Neuroplex software (RedShirtImaging, USA). We captured full frames of 80×80 pixels at readout speeds of 1000, 2000 fps or 3×3 binned at 5000 fps. Before optical recording we focused the microscope on the stained neurons at reduced intensities of excitation. The measured optical signal reflected the change in fluorescence/light emission relative to its mean value ($\Delta F/F$). The data were corrected for bleaching by linear regression. For spatial averaging the neighboring pixels were selected as a region of interest (ROI), and $\Delta F/F$ was calculated as an average light intensity normalized to the resting light intensity acquired before each trial. When needed, the data were filtered with a 3.0 Hz high-pass Butterworth filter to remove slow components of optical signals.

Morphological imaging was performed with AxioCam HR camera mounted on an Axioskop2 microscope equipped with 40×/0.8 N.A. or 20×/0.8 N.A. objectives under control of Axiovision software (Zeiss, Germany). Stacks of confocal images were acquired at 0.6–1 μm step with a LSM 5 Live confocal scanning microscope and 63×/1.0 N.A. W.I., 40×/1.3 N.A. oil, or 20×/0.8 N.A. air objectives (Zeiss, Germany) to either analyze each image individually or produce a detailed 3D-reconstruction. We excited the VSDs with the 532 nm built-in laser (75 mW) and imaged at lowpass emission of 550 nm. We corrected to resting fluorescence by subtracting the background fluorescence value. After the experiments a number of preparations were fixed in 4% paraformaldehyde for 1 h and cleared in glycerol to produce better quality pictures with oil-immersion microscopy. Image stacks were processed off-line by ImageJ software (freeware by NIH, available online at http://rsbweb.nih.gov). For every image the red channel was extracted, and the brightness of each pixel was normalized to the dynamic range of the whole image. Final pictures were created by collapsing the image stacks and merging 3D data into a single plane, or 3D animations were produced.

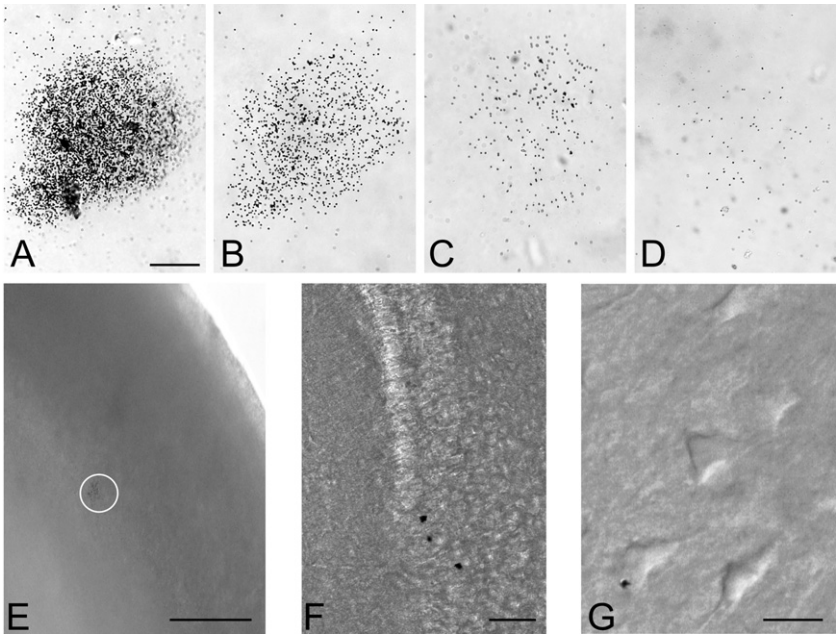

Fig. 2. Dependence of microprojectile densities on the duration of valve open state. To mimic the brain tissue we created non-living targets with 3% agarose gelled in Petri dishes. Distribution of microprojectiles was limited by the outer diameter of biolistic device (150 μm). (A)–(D) Central regions of microprojectile scattering areas are shown for different durations of the valve open state: (A) 300 ms; (B) 100 ms; (C) 50 ms; and (D) 30 ms. (E)–(G) show the distribution of microprojectiles in rat brain slices in the range of increasing magnifications: (E) 0.5×; (F) 10×; and (G) 40×, DIC. Calibration bar in (A)–(D) is 50 μm, (E) 300 μm, (F) 80 μm, and (G) 20 μm. (G) A single microprojectile (black dot) penetrated down to the layer of live neocortical neurons in the slice of visual cortex.

3. Results and discussion

3.1. Biolistic loading of VSDs

Our custom-made biolistic apparatus allowed us to direct microprojectiles coated with the dye precisely to the arbitrarily selected regions of slices sized up to 150 μm in diameter. We used the parameters of delivery selected in the previously published description of the apparatus (Aseyev et al., 2012) that allowed microprojectiles to penetrate the slice down to the depth of 50 μm in depth and were optimal for patch clamp recording and voltage imaging. It was also very important to control the density of the microprojectiles relative to the targeted area. Higher densities (Fig. 2A and B) caused severe damage to the brain tissue and increased the background fluorescence, whereas lower densities decreased the probability to stain the cells at the first trial because

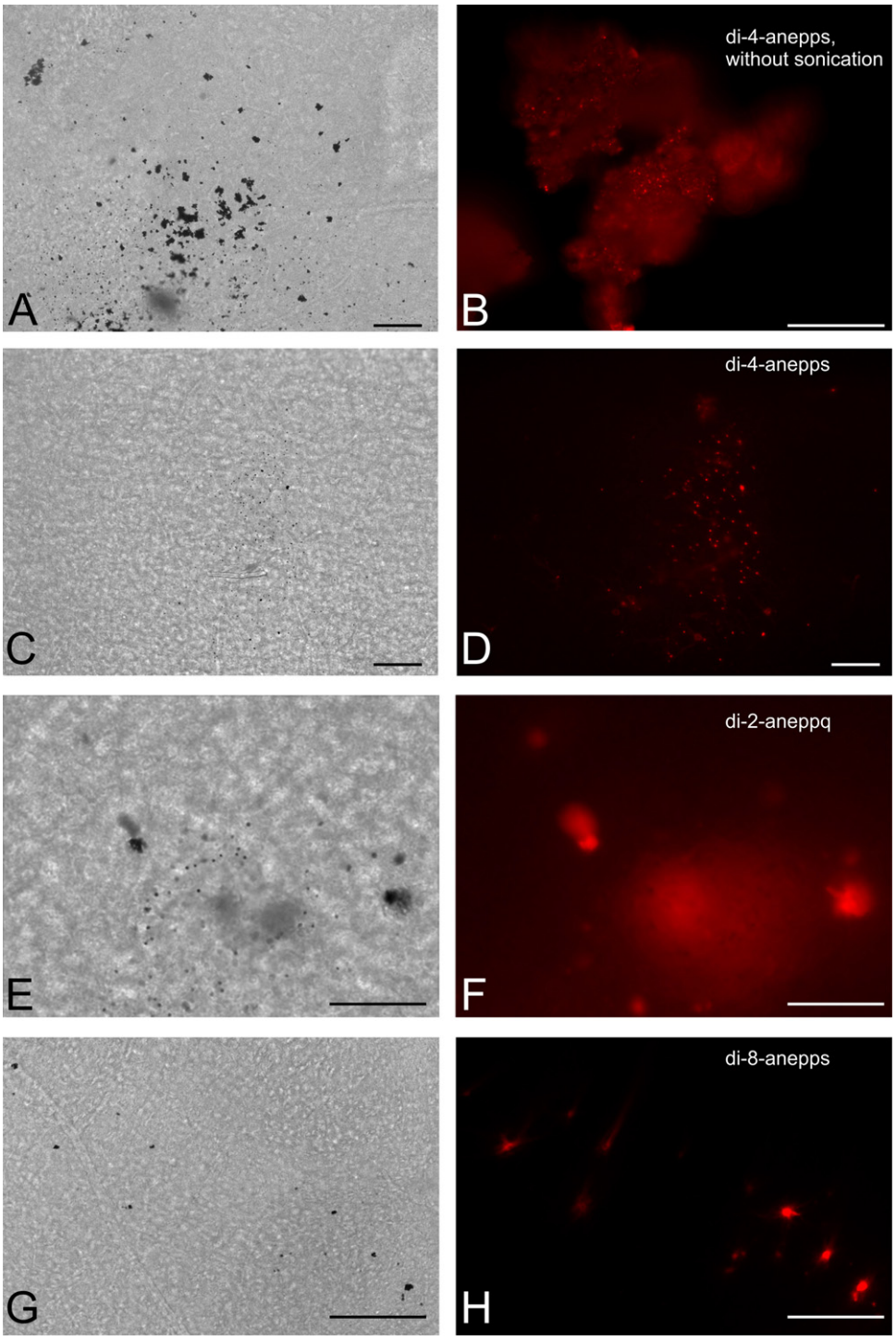

Fig. 3. Delivery patterns of microprojectiles coated with VSDs in rat brain slices. Bright field pictures (left column) and corresponding fluorescent images (right column) from the same area of the slices stained with microprojectiles (except (A) and (B), which are from different preparations). (A and B) Patterns of microprojectiles not subjected to sonication prior to use. The particles tend to aggregate into visibly large conglomerates up to 20 μm. (C and D) Microprojectiles stained with the same dye (di-4-ANEPPS) and the same protocol as in (A) and (B) but treated by ultrasound before use. (E–H) More lipophilic dye shows fewer spills by diffusion in slice and improves the signal-to-noise ratio; (E and F) di-2-ANEPEQ; and (G and H) di-8-ANEPPS. Calibration bars are 50 μm.

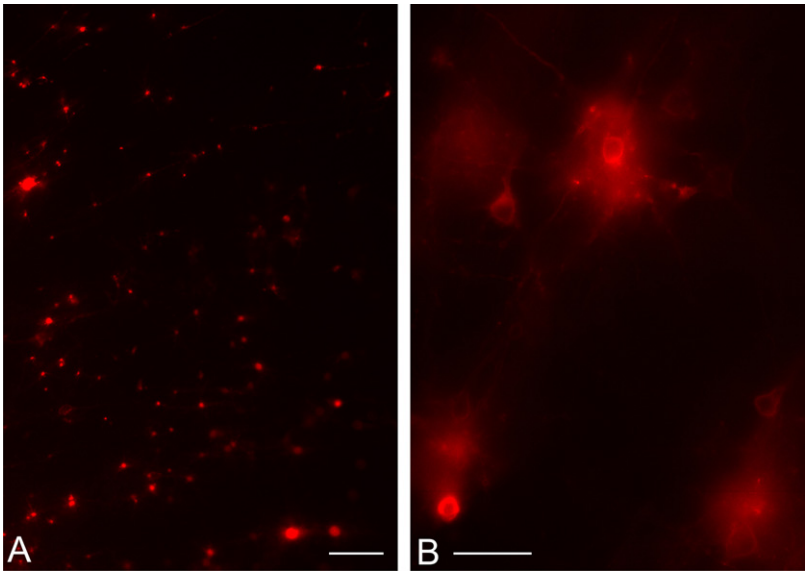

Fig. 4. Scatter patterns of microprojectiles coated with a highly lipophilic fluorescent dye di-12-ANEPPQ. (A) Rare single neurons were imaged at low 5× magnification. The distribution of neurons was nearly even, resembling a classical Golgi-like random pattern. (B) The same stained brain under 20× magnification. Some cells demonstrated small or no background halo around the stained cellular membrane thus providing a possibility to select neurons for voltage imaging with better S/N ratio. Calibration bars 50 μm in (A) and 20 μm in (B).

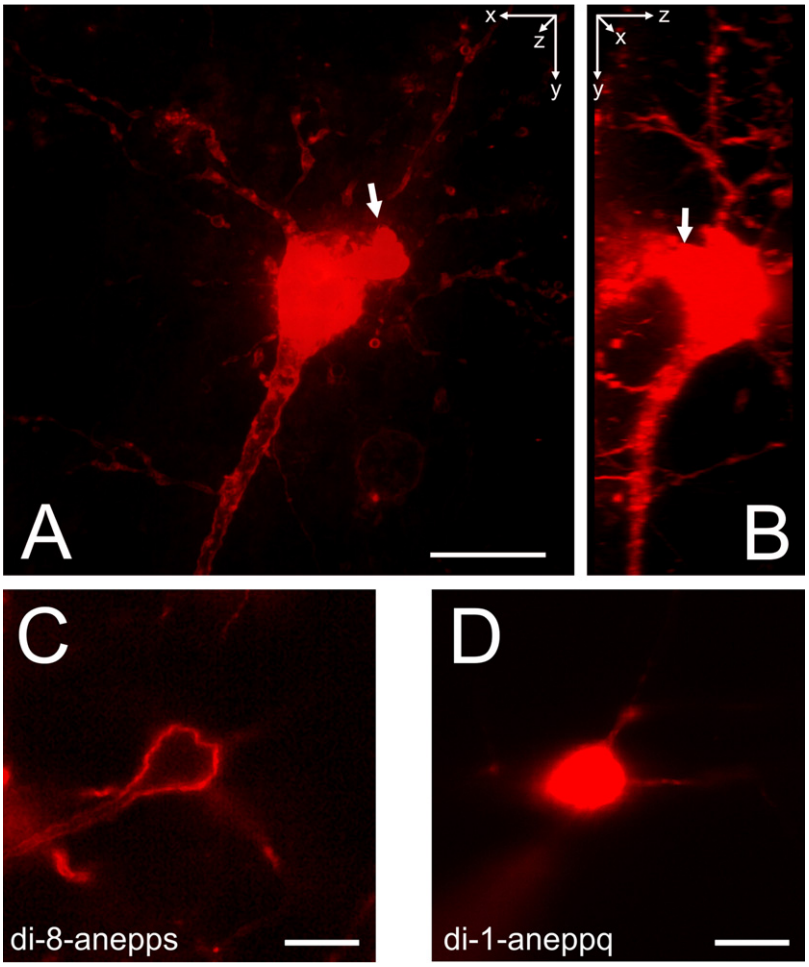

Fig. 5. Confocal imaging of biolistically stained pyramidal neurons of neocortex. Two-dimensional *X*–*Y* (A) and *Y*–*Z* (B) projections of 3D reconstruction (63×/1.0 N.A. lens, stack of 60 frames, step 0.6 μm) with a microprojectile touching the soma of a single neuron (arrows) stained with a lipophilic VSD di-8-ANEPPS. The length of microprojectile's track can be estimated from *Y*–*Z* projection where the right side corresponds to the surface of slice. The micropojectile and its stained surroundings are located below the neuronal soma. (A and B) Calibration bar 20 μm. (C) Optical section of a L5 cortical neuron stained biolistically with a lipophilic VSD di-8-ANEPPS. (D) Optical section of a cortical neuron (L5) stained with an amphiphilic VSD di-1-ANEPPQ through a patch pipette. Estimated thickness of the optical slice is 1 μm with the lens 63×/1 N.A. Membrane potentials of both cells were probed with patch pipettes to make sure they were alive and healthy. (C and D) Calibration bars are 40 μm.

the delivery was a random process depending on the chance and number of microprojectiles penetrating the slice. Densities corresponding to the valve open time of 50 ms (Fig. 2C and D) were acceptable for optical recording and were used in later experiments. DIC images of scatter patterns of microprojectiles in the brain slices are shown in Fig. 2E and F, and an example of a microprojectile located close to the target cells is shown in Fig. 2G.

We modified the protocol used for lipophilic dyes (Gan et al., 2000) to coat microprojectiles with lipophilic VSDs. Microprojectiles coated with VSDs tended to cluster into large conglomerates, especially in high concentrations of the VSD. The optimal concentration (2.5 mg/ml) of dye was found empirically. Splitting conglomerates to individual microbeads by ultrasound was a crucial step to achieve consistent patterns of scattering. Fig. 3 (A and B versus C and D) shows how sonication of coated microprojectiles broke the conglomerates and dramatically improved their scattering. Conglomerates of microprojectiles coated with di-2-ANEPEQ were more difficult to break due to the amphiphilic properties of the dye that resulted in removal of the microprojectiles' coating during sonication in water. For this reason we used an homogenization by manually applied pestle followed by a centrifugation of obtained powder for the di-2-ANEPEQ-coated microprojectiles. This procedure appeared to be less effective than sonication as there apparently remained some minor conglomerates of microprojectiles.

We tested 4 ANEP-based VSDs with varying lipophilic properties to find the best candidate for staining of live neurons in the acute brain slices (Fig. 3, E and F versus G and H). The two most hydrophilic dyes, di-2-ANEPEQ and the slightly less hydrophylic di-4-ANEPPS, were found inappropriate because the water solubility of these dyes permitted them to diffuse through the extracellular space and thereby significantly increased the background fluorescence. In contrast, after delivery of microprojectiles coated with more lipophilic dyes di-8-ANEPPS and di-12-ANEPPQ, we observed much smaller or no dye leakage into the extracellular space, and Golgi-like staining patterns with randomly located and rarely stained neurons on clear backgrounds (Figs. 3E–H and 4). These results promised a minimal noise from background fluorescence, thus optimizing the signal for functional imaging.

We acquired *Z*-stacks of confocal images to visualize morphological types of neurons stained biolistically (Fig. 5). First, we focused on the stained cells with attached microprojectiles using high zoom optics and smaller *Z*-step value of 0.6 μm between individual images in the stacks. An example of a 3D-reconstruction is presented as an animated picture (supplementary video S1). Projections onto two coordinate planes *X*–*Y* and *Y*–*Z* (Fig. 5) demonstrate that a single microprojectile at the somatic compartment of the neuron was able to stain the cell's entire dendritic tree and its axon (Fig. 5A and B). Neurons stained by the dye displayed fluorescence of high intensity. It is well known that the voltage-sensitive dye outside cellular membranes is not affected by the changes of membrane potential, thus decreasing the S/N ratio. Biolistic staining with a lipophilic dye di-8-ANEPPS provided a dye uptake by the membrane only, whereas a conventional procedure of loading through the pipette of the amphiphilic dye di-1-ANEPPQ induced the dye uptake into the cytoplasm as well (Fig. 5C and D).

Using fixed slices and confocal imaging, we visualized different types of neurons stained biolistically (Fig. 6). In our experiments, the fluorescence in cells treated with either di-8-ANEPPS or di-12-ANEPPQ persisted for at least 1 week after staining and fixation. Such a stability of staining pattern may be useful for a more detailed analysis of cell morphology by examining slices of fixed tissue after

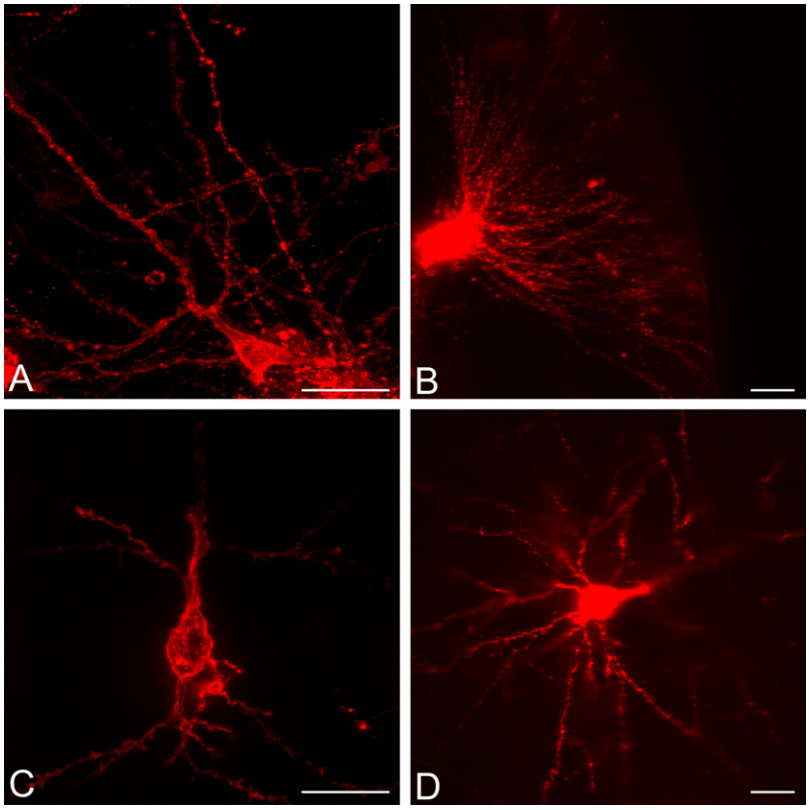

Fig. 6. Fine morphological details of the biolistically loaded neurons revealed by higher resolution confocal microscopy with oil-immersion high N.A. lenses in fixed preparations. Proximal and distal dendrites are evenly stained. (A) L2/3 pyramidal cell of visual neocortex with extensive apical dendrite. (B) Dendritic arbor of a hippocampal pyramidal neuron at CA3 area. (C) Bipolar cell of L2/3 of visual neocortex; (D) L5 large pyramidal neuron of rat visual neocortex. (A and C) 40×/1.3 N.A. lens. (B and D) 20×/0.8 N.A. lens. Calibration bars are 20 μm in all panels.

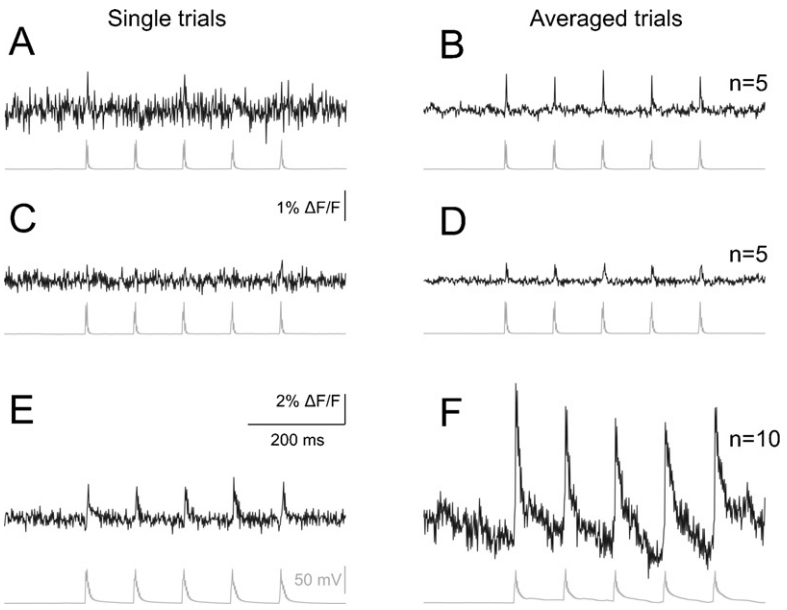

Fig. 7. Comparison of optical traces of single APs averaged within the somatic ROI of the biolistically stained neurons with those loaded through the patch pipette. Left panels, single trials; Right panels, corresponding AP-triggered averaged traces. (A and B) Traces from a neuron loaded through the patch pipette with di-1-ANEPPQ. (C and D) di-8-ANEPPS and (E and F) di-12-ANEPPQ). Top traces in each panel are optical recordings. Gray traces below optical traces are simultaneous current-clamp recordings of the membrane potential. (B and D) Average of 5 trials recorded at 1000 fps and (F) average of 10 trials recorded at 5000 fps.

the physiological experiment under a confocal microscope where oil-immersion objectives that provide better optical resolution can replace the water-immersion objectives used for fast imaging due to much higher N.A.

The cells showed different levels of fluorescence depending on the cell part contacted by the microprojectile and on the amount of dye carried by the particle. It proved difficult to measure the speed of dye diffusion along the cell membranes within the areas available for observation. With the employed methods of imaging it was impossible to detect any difference in staining of the distant neurites (located at 5 sizes of soma distance) observed at the 10-th or 30-th min after the VSD delivery within the field of view (~200 μm with 63× lens). A small increase in background fluorescence around the stained cells was observed after 2 h of incubation, indicating very slow leakage of the dye from the membrane.

The previously reported speed of retrograde loading of the employed lipophilic dyes ranged from 1 h to 1 day of incubation in order to stain the soma of a ganglionic motoneuron by dye loading though its axon in the nerve (Wenner et al., 1996). The distances for the dye to travel in the spinal cord preparations (0.5–1 mm) used for retrograde loading might be affected by the surfactants used to dissolve the dye. Hydrophilic VSDs also need a significant time to spread to the cell's neurites (up to 1 h, plus 1–2 h incubation; Antic et al., 1999). Even the fastest known red dye, di-1-ANEPEQ (most commonly referred as JPW3028), requires more time of incubation for staining of the distal dendrites when applied through the patch pipette: from 1.5 h (Zhou et al., 2007) up to 3 h (Antic et al., 1999) after the removal of patch pipette. The time issue is very important because besides the voltage-sensitivity, the speed with which a voltage-sensitive dye diffuses through the intracellular space is perhaps the major feature to determine its usefulness in experiments (Zhou et al., 2007). These authors measured the speed of staining in pyramidal neurons of cortical brain slices with the recent generation of VSDs ("blue dyes", e.g. di-1-APEFEQPQ; Wuskell et al., 2006), which have the red excitation wavelengths up to 700 nm and infrared emission spectra extending to 900 nm. In simple staining experiments with proximal dendrite imaging the minimal time of staining for successful optical recording was reported to be less than 60 min (Zhou et al., 2007).

The technique of biolistic delivery was introduced to transfect the cells, i.e. a microprojectile with an attached plasmid vector must penetrate the cell, and the transfected cell must now recover and survive at least 24 h to express the RNA product (Sanford, 1988;

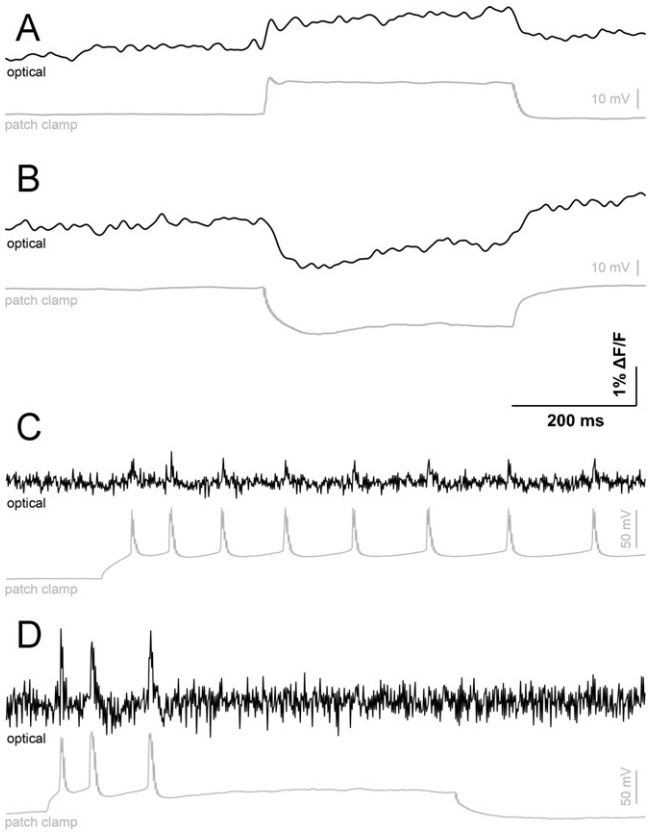

Fig. 8. Single optical traces of somatic ROIs of the neurons biolistically stained with di-12-ANEPPQ. (A and B) Subthreshold responses to 200 pA current steps. (C and D) APs evoked by long 500 pA current steps. Gray traces below optical traces are simultaneous current-clamp recordings of the membrane potential. (C) Staining through a patch pipette with di-1-ANEPPQ for comparison.

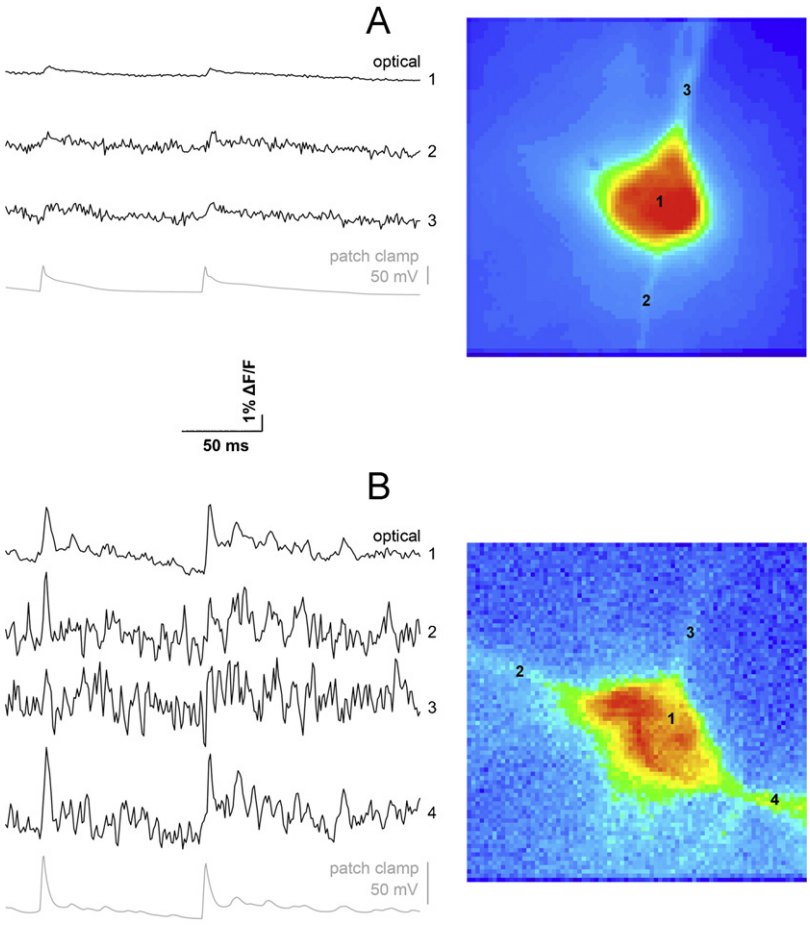

Fig. 9. Optical signals obtained from the cellular compartments of neurons stained intracellularly through a patch pipette with di-1-ANEPPQ (A), and biolisticaly with di-12-ANEPPQ (B). Gray traces below optical traces are simultaneous current-clamp recordings of the membrane potential. Photomicrographs of the neurons and their neurites are shown on the right sides of each panel. Sites of voltage imaging are indicated with numbers corresponding to the optical traces on the left. Further improvement of S/N ratio is possible with lower readout noise CCDs or brighter light sources like a low ripple noise laser or superbright LED.

Johnston, 1990). Biolistic delivery was successfully adopted for the imaging of intracellular calcium transients of single neurons in brain slices and whole brains (Kettunen et al., 2002). It suggests that the biolistically labeled neurons are still functional with preserved intracellular machinery to maintain the protein composition and a possibility to react to biologically relevant stimuli. One possible way to reduce the harmful impact of the microprojectiles on the tissue is to employ smaller nano-scale sized carriers (Lian et al., 2007; O'Brien and Lummis, 2011). We used relatively big microprojectiles (1.6 μm in diameter) which are in average only 10 times smaller than the somatic size of the neurons in rat visual cortex (5–20 μm), assuming that a microbead can do some harm in unlucky cases, and such cases were observed during detailed examination of stained cells. It is possible that the damage will be reduced upon adaptation of the staining protocols with nano-carriers to the VSDs.

3.2. Optical recording of voltage in biolistically stained neurons

To demonstrate the effectiveness of biolistic delivery of VSDs for the purpose of membrane potential imaging, we performed simultaneous electrophysiological and optical recordings of the activity of brain slice neurons stained biolistically with di-8-ANEPPS or di-12-ANEPPQ. We patched 14 biolistically stained neurons. In 5 of 14 patched neurons the membrane potential was lower than −50 mV. Control optical responses were recorded with the conventional loading of di-1-ANEPPQ through the patch pipette and the same parameters of stimulation current (3 cells) for comparison. We applied very short (2 ms) and relatively strong current steps (1–2 nA) to the recorded cells to evoke APs. Stimulation was adjusted to evoke up to 100 mV potential peak in current clamp mode. In these experiments the current steps were automatically applied in trains of 5 with 100 ms interstimulus intervals. The AP served as a trigger to average the trials online.

Both biolistically delivered and patch-loaded dyes demonstrated considerable signals and changes in fluorescence ($\Delta F/F$) in response to current-evoked APs and subthreshold depolarization steps (Figs. 7 and 8). The optical signal induced by a single AP in the soma of pyramidal neurons stained with di-12-ANEPPQ was 3.6 ± 1.2 $\Delta F/F$ ($n = 4$ cells, S/N ~ 1–5) and that in the dendrites was 6.4 ± 1.7 ($n = 3$ cells). This is comparable to the AP-associated signal obtained with a similar xenon-lamp powered illumination system in basal dendrites (3–4%; Antic, 2003). A slightly higher signal obtained in the dendrites in our experiments can be explained by the lack of internalization of a highly lipophilic dye di-12-ANEPPQ together with the doubled membrane contribution in the dendrite comparing to a single membrane layer in the focal plane at the somatic ROI. In our experiments the averaged $\Delta F/F$ of the dye loaded through patch pipette was 0.5 ± 0.2 ($n = 3$ cells) in the soma and 1.2 ± 0.4 ($n = 3$ cells) in the dendrites. This is significantly smaller that $\Delta F/F$ in the experiments with biolistic delivery (ANOVA, $p < 0.05$) although higher values of $\Delta F/F$ for intracellularly loaded dyes had been reported in the literature (Antic, 2003; Foust et al., 2010; Popovic et al., 2011). Interestingly, the sign of $\Delta F/F$ was the same both in biolistic and intracellular staining experiments

suggesting that the biolistically delivered dye also stains the neuronal membrane from the inside.

We compared the biolistic delivery and patch application of the VSDs by analyzing optical trials with similar recording parameters but with different dyes and delivery techniques used (Fig. 9). In general, the amount of dye that reached the cell membrane with biolistic technique is apparently smaller than by staining with intracellular injection. S/N ratio of AP-associated optical signals at Fig. 9A (patch delivery) is roughly equal to one; while at Fig. 9B (biolistic) is ~1–4. When comparing relative changes in fluorescence ($\Delta F/F$) per compartment (averaged from many pixels, similar for both cases) for these two records, it was clear that signal amplitude is higher in B (biolistic). This is in agreement with the evaluation of ANEP dyes sensitivity by population signals from ganglia motoneurons (Tsau et al., 1996; Wenner et al., 1996). From this work the better S/N ratio was expected for highly lipophilic ANEP VSDs then for intracellularly used water soluble ones. In our experiments, we observed relatively poor S/N ratio for di-12-ANEPPQ, probably because of a relatively lower dye amount delivered biolistically to the cell. It is possible to further improve the S/N ratio by using highly sensitive EM-CCD camera with appropriate low noise excitation, improving the excitation intensity (LED or low-noise laser), and using higher N.A. lenses.

The major advantages of biolistic delivery of VSDs are: (1) a possibility to employ highly lipophilic dyes of high sensitivity and good S/N ratio; (2) no need for complicated and long procedures of repatching, also the cytoplasmic content is preserved after biolistic staining; (3) complicated patch clamp equipment and infrared DIC optics are not necessarily required for voltage imaging; and (4) short duration of biolistic staining may positively contribute to the condition of preparation in acute imaging experiments. Moreover, the biolistic delivery can be potentially used in whole brains of intact animals.

It is important to note that voltage imaging with biolistic delivery of the VSD is a difficult kind of experiment with several disadvantages: (1) custom-made equipment required with the adjustments to a specific preparation; (2) possible damage to live tissues with biolistic shot which can even kill some cells in the slice (however, many cells are stained, so the researcher can select good ones for optical recording); and (3) pre-selection of specific cell types in a nonhomogeneous population is not possible due to stochastic neuronal staining patterns within the targeted area.

4. Conclusions

We successfully used the biolistic delivery of hydrophobic VSDs to the membranes of live neurons. This technique permitted the rapid staining of random single neurons in acute brain slices. Hydrophobic dyes di-12-ANEPPQ and di-8-ANEPPS stained the neuronal soma, dendrites and axon to a level of fluorescence suitable for optical recording with a fast CCD camera. The biolistic delivery can be potentially employed to record individual neurons in the intact animal brain.

Acknowledgements

We thank Dr. Dmitry A. Rinberg (HHMI Janelia Farm) who inspired this study, Dr. Leslie M. Loew (University of Connecticut) for di-12-ANEPPQ and di-1-ANEPPQ samples, Dr. Alexey Malyshev (IHNA RAS) for his advices and productive discussion of the work. We are grateful to Dr. Richard Boyle for comments on manuscript and editing. This study was supported by Federal Grant-in-Aid Program "Human Capital for Science and Education in Innovative Russia" (Federal Targeted Program "Scientific and Scientific-Pedagogical Personnel of the Innovative Russia in 2009–2013" Contract P330 NK-542P/40, contract P608), grant of RF President Council for Grants to PMB, Russian Academy of Sciences Programs: Molecular and Cell Biology, Fundamental Sciences to Medicine, Integrative Physiology.

Appendix A. Supplementary data

Supplementary data associated with this article can be found, in the online version, at http://dx.doi.org/10.1016/j.jneumeth.2012.09.008.

References

Acker CD, Yan P, Loew LM. Single-voxel recording of voltage transients in dendritic spines. Biophys J 2011;101:L11–3.
Antic S, Major G, Chen WR, Wuskel J, Loew L, Zecević D. Fast voltage-sensitive dye recording of membrane potential changes at multiple sites on an individual nerve cell in the rat cortical slice. Biol Bull 1997;193(October (2)):261.
Antic S, Major G, Zecevic D. Fast optical recordings of membrane potential changes from dendrites of pyramidal neurons. J Neurophysiol 1999;82:1615–21.
Antic SD. Action potentials in basal and oblique dendrites of rat neocortical pyramidal neurons. J Physiol 2003;550:35–50.
Aseyev N, Nikitin ES, Roshchin MV, Ierusalimsky VN, Balaban PM. Fast and aimed delivery of voltage-sensitive dyes to mammalian brain slices by biolistic techniques. Zh Vyssh Nerv Deiat Im I P Pavlova 2012;62:100–7.
Ballanyi K. In vitro preparations. In: Johanson H, Windhorst U, editors. Modern techniques in neuroscience research. Heidelberg: Springer-Verlag; 1999. p. 307–26.
Bouevitch O, Lewis A, Pinevsky I, Wuskell JP, Loew LM. Probing membrane potential with nonlinear optics. Biophys J 1993;65:672–9.
Canepari M, Zecevic D. Membrane potential imaging in the nervous system: methods and applications. New York: Springer; 2010.
Cohen LB. More light on brains. Nature 1988;331:112–3.
Cohen LB, Salzberg BM. Optical measurement of membrane potential. Rev Physiol Biochem Pharmacol 1978;83:35–88.
Foust AJ, Popovic M, Zecevic D, McCormick DA. Action potentials initiate in the axon initial segment and propagate through axon collaterals reliably in cerebellar Purkinje neurons. J Neurosci 2010;30(20):6891–902.
Foust AJ, Yu Y, Popovic M, Zecevic D, McCormick DA. Somatic membrane potential and Kv1 channels control spike repolarization in cortical axon collaterals and presynaptic boutons. J Neurosci 2011;31:15490–8.
Gan WB, Grutzendler J, Wong RO, Lichtman JW. Ballistic delivery of dyes for structural and functional studies of the nervous system. Cold Spring Harb Protoc 2009(4):1–10, http://dx.doi.org/10.1101/pdb.prot5202, pdb.prot5202.
Gan WB, Grutzendler J, Wong WT, Wong RO, Lichtman JW. Multicolor DiOLISTIC labeling of the nervous system using lipophilic dye combinations. Neuron 2000;27:219–25.
Grinvald A, Salzberg BM, Lev-Ram V, Hildesheim R. Optical recording of synaptic potentials from processes of single neurons using intracellular potentiometric dyes. Biophys J 1987;51(4):643–51.
Johnston SA. Biolistic transformation: microbes to mice. Nature 1990;346:776–7.
Kettunen P, Demas J, Lohmann C, Kasthuri N, Gong Y, Wong RO, et al. Imaging calcium dynamics in the nervous system by means of ballistic delivery of indicators. J Neurosci Methods 2002;119:37–43.
Kralj JM, Douglass AD, Hochbaum DR, Maclaurin D, Cohen AE. Optical recording of action potentials in mammalian neurons using a microbial rhodopsin. Nat Methods 2012;9:90–5.
Lian WN, Chang CH, Chen YJ, Dao RL, Luo YC, Chien JY, et al. Intracellular delivery can be achieved by bombarding cells or tissues with accelerated molecules or bacteria without the need for carrier particles. Exp Cell Res 2007;313:53–64.
Lichtman JW, Livet J, Sanes JR. A technicolour approach to the connectome. Nat Rev Neurosci 2008;9:417–22.
Miller EW, Lin JY, Frady EP, Steinbach PA, Kristan Jr WB, Tsien RY. Optically monitoring voltage in neurons by photo-induced electron transfer through molecular wires. Proc Natl Acad Sci USA 2012;109:2114–9.
Morgan JL, Kerschensteiner D. Shooting DNA, dyes, or indicators into tissue slices using the gene gun. Cold Spring Harb Protoc 2011;2011:1512–4.
Nishimura M, Shirasawa H, Song WJ. A light-emitting diode light source for imaging of neural activities with voltage-sensitive dyes. Neurosci Res 2006;54:230–4.
O'Brien JA, Holt M, Whiteside G, Lummis SC, Hastings MH. Modifications to the handheld Gene Gun: improvements for in vitro biolistic transfection of organotypic neuronal tissue. J Neurosci Methods 2001;112:57–64.
O'Brien JA, Lummis SC. Nano-biolistics: a method of biolistic transfection of cells and tissues using a gene gun with novel nanometer-sized projectiles. BMC Biotechnol 2011;11:66.
Obaid AL, Koyano T, Lindstrom J, Sakai T, Salzberg BM. Spatiotemporal patterns of activity in an intact mammalian network with single-cell resolution: optical studies of nicotinic activity in an enteric plexus. J Neurosci 1999;19:3073–93.
Palmer LM, Stuart GJ. Site of action potential initiation in layer 5 pyramidal neurons. J Neurosci 2006;26:1854–63.
Palmer LM, Stuart GJ. Membrane potential changes in dendritic spines during action potentials and synaptic input. J Neurosci 2009;29(21):6897–903.
Peterka DS, Takahashi H, Yuste R. Imaging voltage in neurons. Neuron 2011;69:9–21.

Popovic MA, Foust AJ, McCormick DA, Zecevic D. The spatio-temporal characteristics of action potential initiation in layer 5 pyramidal neurons: a voltage imaging study. J Physiol 2011;589(Pt 17):4167–87.
Rinberg DA, Simmonet C, Groisman A. Pneumatic capillary gun for ballistic delivery of microparticles. Appl Phys Lett 2005;87:014103.
Ross WN, Reichardt LF. Species-specific effects on the optical signals of voltage-sensitive dyes. J Membr Biol 1979;48:343–56.
Rohr S, Salzberg BM. Multiple site optical recording of transmembrane voltage (MSORTV) in patterned growth heart cell cultures: assessing electrical behavior, with microsecond resolution, on a cellular and subcellular scale. Biophys J 1994;67(September (3)):1301–15.
Sanford JC. The biolistic process. Trends Biotechnol 1988;6:299–302.
Seabold GK, Daunais JB, Rau A, Grant KA, Alvarez VA. DiOLISTIC labeling of neurons from rodent and non-human primate brain slices. J Vis Exp 2010;41:e2081.
Shefi O, Simonnet C, Baker MW, Glass JR, Macagno ER, Groisman A. Microtargeted gene silencing and ectopic expression in live embryos using biolistic delivery with a pneumatic capillary gun. J Neurosci 2006;26:6119–23.
Sinha S, Saggau P. Optical recording from populations of neurons in brain slices. In: Johanson H, Windhorst U, editors. Modern techniques in neuroscience research. Heidelberg: Springer-Verlag; 1999. p. 459–86.
Stein W, Stadele C, Andras P. Optical imaging of neurons in the crab stomatogastric ganglion with voltage-sensitive dyes. J Vis Exp 2011;49:e2567.
Theer P, Denk W, Sheves M, Lewis A, Detwiler PB. Second-harmonic generation imaging of membrane potential with retinal analogues. Biophys J 2011;100:232–42.
Tominaga T, Tominaga Y, Yamada H, Matsumoto G, Ichikawa M. Quantification of optical signals with electrophysiological signals in neural activities of di-4-ANEPPS stained rat hippocampal slices. J Neurosci Methods 2000;102:11–23.
Tsau Y, Wenner P, O'Donovan MJ, Cohen LB, Loew LM, Wuskell JP. Dye screening and signal-to-noise ratio for retrogradely transported voltage-sensitive dyes. J Neurosci Methods 1996;70:121–9.
Vignali S, Peter N, Ceyhan G, Demir IE, Zeller F, Senseman D, et al. Recordings from human myenteric neurons using voltage-sensitive dyes. J Neurosci Methods 2010;192:240–8.
Volgushev MA, Malyshev A, Nikitin ES. Temperature dependence of action potential initiation in neocortical neurons and conductance based models. Soc Neurosci Abstr 2011, 239.11/D56.
Volgushev M, Vidyasagar TR, Chistiakova M, Yousef T, Eysel UT. Membrane properties and spike generation in rat visual cortical cells during reversible cooling. J Physiol 2000;522(Pt 1):59–76.
Wenner P, Tsau Y, Cohen LB, O'Donovan MJ, Dan Y. Voltage-sensitive dye recording using retrogradely transported dye in the chicken spinal cord: staining and signal characteristics. J Neurosci Methods 1996;70:111–20.
Wu JY, Lam YW, Falk CX, Cohen LB, Fang J, Loew L, et al. Voltage-sensitive dyes for monitoring multineuronal activity in the intact central nervous system. Histochem J 1998;30:169–87.
Wuskell JP, Boudreau D, Wei MD, Jin L, Engl R, Chebolu R, et al. Synthesis, spectra, delivery and potentiometric responses of new styryl dyes with extended spectral ranges. J Neurosci Methods 2006;151:200–15.
Zhou WL, Yan P, Wuskell JP, Loew LM, Antic SD. Intracellular long-wavelength voltage-sensitive dyes for studying the dynamics of action potentials in axons and thin dendrites. J Neurosci Methods 2007;164:225–39.